International Journal of Multiphase Flow 35 (2009) 617–627

Contents lists available at ScienceDirect

International Journal of Multiphase Flow

journal homepage: www.elsevier.com/locate/ijmulflow

Primary instabilities of liquid film flow sheared by turbulent gas stream

S.V. Alekseenko [a,b], S.P. Aktershev [a], A.V. Cherdantsev [a,b,*], S.M. Kharlamov [a], D.M. Markovich [a,b]

[a] Institute of Thermophysics, Siberian Branch of Russian Academy of Science, Lavrentiev ave., 1, Novosibirsk 630090, Russian Federation
[b] Novosibirsk State University, Pirogov str., 2, Novosibirsk 630090, Russian Federation

ARTICLE INFO

Article history:
Received 24 August 2008
Received in revised form 19 January 2009
Accepted 11 March 2009
Available online 20 March 2009

Keywords:
Liquid film
Gas shear
Annular flow
Linear stability
Linear waves
Dispersion relations

ABSTRACT

Evolution of excited waves on a viscous liquid film has been investigated experimentally for the annular gas–liquid flow in a vertical tube. For the first time the dispersion relations are obtained experimentally for linear waves on liquid film surface in the presence of turbulent gas flow. Both cocurrent and countercurrent flow regimes are investigated. As an example of comparison with theory, the experimental data are compared to the results of calculations based on the Benjamin quasi-laminar model for turbulent gas flow. The calculation results are found to be in good agreement with experiments for moderate values of film Reynolds number.

1. Introduction

Joint motion of gas and liquid film takes place in different apparatuses used in power industry and chemical technology. Interface waves significantly affect the intensity of heat and mass transfer processes, and study of wave formation is an important problem for practical applications. Apart from practical significance, the problem of wave regimes of film flow is of general fundamental interest as an example of nonlinear waves in a system with dissipation and energy pumping.

Numerous experimental and theoretical studies were dedicated to the problem of stability for free falling films, starting with pioneer works of Kapitza (1948) and Benjamin (1957). This problem was extensively investigated in the 1960–1980s. Experiments performed by, among others, Krantz and Goren (1971), Pierson and Whitaker (1977) demonstrated that the phase velocity and increment of growing waves are satisfactorily described by linear stability theory. To date the problem of the primary instability for a free falling film has been studied in detail (Alekseenko et al., 1994; Chang and Demekhin, 2002) and now attention is generally drawn to the experimental and theoretical study of different forms of the secondary instabilities of film flow (Liu et al., 1993; Cheng and Chang, 1995; Liu et al., 1995; Vlachogiannis and Bontozoglou, 2001; Chang and Demekhin, 2002).

The existence of gas flow over the liquid film results in appearance of the shear and normal stresses on the gas–liquid interface, which are crucial for film stability and characteristics of generated waves. Modeling of such flow is a rather complicated problem. A series of consequent simplifying assumptions are usually used. The main assumption is the approach of "divided attack", allowing deriving equations for gas and liquid flow separately (Benjamin, 1957, 1959; Miles, 1959). This approach was applied for investigation of stability of gas sheared liquid films using Orr–Sommerfeld equation (Guguchkin et al., 1979; Chan Van Chan and Shkadov, 1979; van Gastel et al., 1985; Jurman and McCready, 1989; Demekhin et al., 1989; Aktershev and Alekseenko, 1996; Miesen and Boersma, 1995) or integral approach (Hanratty, 1983; Alekseenko and Nakoryakov, 1995).

Different model assumptions were suggested by various researchers, considering velocity profiles in liquid and gas phase, shear and normal stresses variations on free surface. A considerable number of papers are devoted to reciprocal comparison of the results obtained with the use of such assumptions (e.g., van Gastel et al., 1985; Kuru et al., 1995; Miesen and Boersma, 1995; Inada et al., 2004). Comparison with experimental results is usually fragmentary; the theoretical curves are often compared to 1–2 measured experimental points. The reason for such incomplete comparison is the lack of experimental data on wave characteristics of linearly developing waves in a wide frequency range for the case of gas sheared liquid films.

In obtaining such data the main difficulty is that the waves which are close to linear and associated with primary instability of film surface quickly evolve into groups of nonlinear 2D and 3D waves with unstable parameters having a tendency to change with distance from the place of origin. The evolution scenario may vary greatly, depending on liquid and gas flow rates, channel

* Corresponding author. Address: Novosibirsk State University, Pirogov str., 2, Novosibirsk 630090, Russian Federation. Tel.: +7 3833325678; fax: +7 3833356684.
E-mail address: cherdantsev@itp.nsc.ru (A.V. Cherdantsev).

0301-9322/$ - see front matter © 2009 Elsevier Ltd. All rights reserved.
doi:10.1016/j.ijmultiphaseflow.2009.03.003

orientation, etc. (Semenov, 1944, Hanratty and Engen, 1957; Rossum, 1959; Lilleleht and Hanratty, 1961; Smith and Tait, 1966; Stainthorp and Batt, 1967; Cohen and Hanratty, 1968; Craik, 1966; Guguchkin et al., 1975). In numerous experimental works the different wavy flow modes (two-dimensional close-to-sinusoidal waves, three-dimensional "pebble-shaped" waves, soliton-like "rolling" waves, "slow" waves with the velocity lower than that of the interface, etc.) have been identified and mapped, and the parameters of these waves (amplitude, shape, wavelength, and phase velocity) were measured and plotted as functions of flow parameters.

Despite of importance of obtained wave parameters for description of the flow, they are unsuitable for comparison with stability theories, since the latter describe primary instability and do not consider further development of wavy motion into different wavy modes.

The connection between primary and secondary instability is often simplified, assuming that stationary nonlinear waves directly evolve from primary waves of maximum growth. But experimental data on stationary waves are inconsistent with theoretical parameters of waves of maximum growth. For example, Asali and Hanratty (1993) obtained experimental wavelengths two times higher than those predicted for waves of maximum growth. Authors suggested that the discrepancy might be explained by the secondary instability in transversal direction.

A possible way to measure the parameters of primary instability experimentally is the statistical treatment of film thickness records in the region of linear growth of waves (as done in the work of Pierson and Whitaker (1977) for free falling film). However, this approach gives essential scattering of experimental data due to a number of experimental difficulties (small size of area of linear growth, small amplitude of linear waves, high level of noise, etc.).

More reliable experimental data on primary instability may be obtained in deterministic approach, by investigating evolution of artificially exited harmonic waves in a wide range of excitation frequencies. The measured values of increment of amplitude growth and phase velocity of excited waves obtained for the whole range of excitation frequencies give the dispersion dependencies characterizing primary instability properties. These dependencies could be used for direct comparison with different theoretical assumptions. Similar deterministic approach was also used by Krantz and Goren (1971) for experimental investigation of stability of gravitationally-driven liquid films as well as in recent work of Tsai et al. (2005), who investigated excited waves on deep water surface under gas shear.

The present work is devoted to experimental obtaining the dispersion dependencies for artificially excited linear waves on the surface of annular film sheared by both cocurrent and countercurrent turbulent gas flow. For illustrative comparison of our experimental dependencies with theory, linear stability theory based on Orr–Sommerfeld equation was chosen. In the model equations shear and normal stress variations calculated by Demekhin (1981) are used. This model is described in detail in Aktershev and Alekseenko (1996), and its short description is given in Appendix A. To estimate the influence of certain factors (the channel curvature, the possible hydrodynamic stabilization of film flow in the region of measurement, existence of low-frequency external vibrations) on dispersion dependencies, integral approach is used. This approach is presented by Alekseenko et al. (1994) and Alekseenko and Nakoryakov (1995).

2. Experiments description

2.1. Experimental setup and flow parameters

The wave characteristics were measured for a film flowing on the inner surface of a vertical Plexiglas tube with an inner diameter of 15 mm and length of 1 m (see Fig. 1). Fig. 2 shows the area of measurements near the inlet region of film flow. The film is blown by air that is fed through a reduction gear from a compressed air pipeline. The air is supplied through thin stainless steel tubes installed on the top and at the bottom of the working section coaxially to the main pipe. The inner diameter of the top tube for air feeding (which provides the air flow cocurrent to the film flow) is 13.4 mm and its wall thickness is 0.3 mm. The tube for formation of the countercurrent flow has the inner diameter of 9 mm. The working liquid was distilled water or water–glycerin solutions of different viscosity with addition of NaCl (0.1% by mass). The liquid is supplied from the overhead tank, then passes through the flowmeter and stabilizing section and is fed to the working section through an annular gap between the external surface of upper air-feeding tube and the inner surface of the Plexiglas pipe. The gap is of 0.5 mm width and 60 mm length. The waves of prescribed frequency and amplitude are formed under the action of flexible oscillating membrane, which is installed at the inlet of the stabilization chamber and is driven by electromagnetic vibrator controlled by a harmonic signal from the low-frequency generator. The liquid properties and tested regimes are listed in Table 1. The negative values of superficial gas velocity refer to the countercurrent flow. Since tube diameter and physical properties of gas did not change in our experiments, the Reynolds number for gas phase is directly proportional to the absolute value of superficial gas velocity. Thus, $V_g = \pm 5.1$ m/s corresponds to $Re_g = 5100$; $V_g = \pm 7.3$ m/s – to $Re_g = 7300$; $V_g = \pm 8$ m/s – to $Re_g = 8000$.

2.2. Measurement technique

The characteristics of waves are measured by conductivity sensors flash-mounted into the pipe wall. Sensors of this type are widely used for film flow study (see, e.g., Chu and Dukler

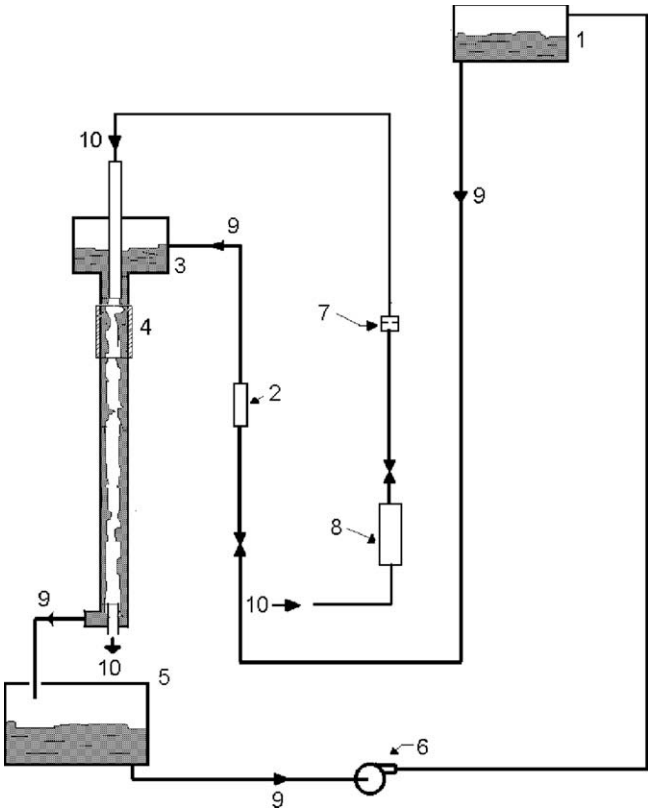

Fig. 1. Layout of the test facility. 1 – feeding tank; 2 – liquid flowmeter; 3 – distributor; 4 – conductivity sensors; 5 – receiving tank; 6 – pump; 7 – air flowmeter; 8 – reducer and filter; 9 – hydraulic line; 10 – air line.

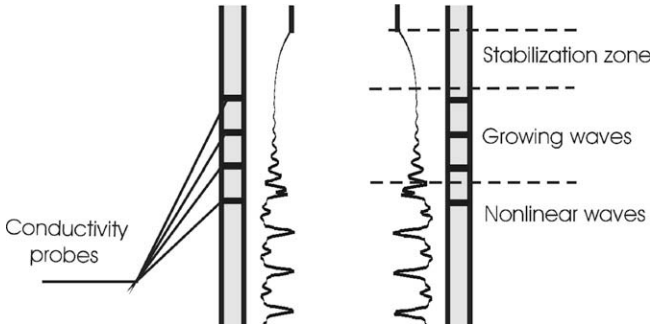

Fig. 2. Location of the probes relative to inlet region of film flow.

(1974)). The experimental data on film thickness are recorded by four-channel facilities using the conductivity sensors with coaxial electrodes. All four sensors are identical and have the following parameters: the diameter of the central electrode is 2 mm; the thickness of insulation gap between the central electrode and the shell – 2 mm; the distance between adjoined sensors – 15 mm; the frequency of feed voltage is 10 kHz; and the bandwidth at the demodulator outlet is 0–1000 Hz. The output signal of demodulator is transmitted to the PC-plugged 12-bit ADC, then quantized with the sampling frequency of 5 kHz and stored to a hard drive. The primary calibration of sensors was performed by creation of annular gaps of different widths in the channel filled with working liquid. The stability of calibration dependence during experiments was ensured by periodic measurements of free falling film thickness at several fixed liquid flow rates. The two-channel recording of local film thickness at fixed liquid flow rate and different air velocities are shown in Fig. 3. As can be seen, for fixed location of the sensors nonlinear transformation of the waves strongly depends on the velocity of gas flow. Procedure of determination the downstream distances where waves may be regarded as linear ones is described in the next section.

Preliminary testing was carried out using three sensors spread at the transversal angle of 120° relative to each other. This test showed that excited waves are two-dimensional.

The signal was processed in spectral domain. Dimensionless phase velocity of waves and dimensionless spatial increment of waves amplitude were calculated as:

$$c = 2\pi fL/(\varphi_1 - \varphi_2)u_0,$$
$$\alpha = \ln(A_2/A_1) \times (h_0/L),$$

where ϕ_1, ϕ_2 and A_1, A_2 are the phases and amplitudes of the first harmonic for film thickness records registered by two adjacent probes. L is the distance between probes, f is the frequency of excited wave, $h_0 = (3\nu^2\mathrm{Re}/g)^{1/3}$, and $u_0 = gh_0^2/3\nu$, are the thickness and superficial velocity for equilibrium smooth film by Nusselt. Here g is the gravitation acceleration, ν – kinematic viscosity of liquid, Re – Reynolds number of film flow defined as q/ν, q – volumetric liquid flow rate per unit film width.

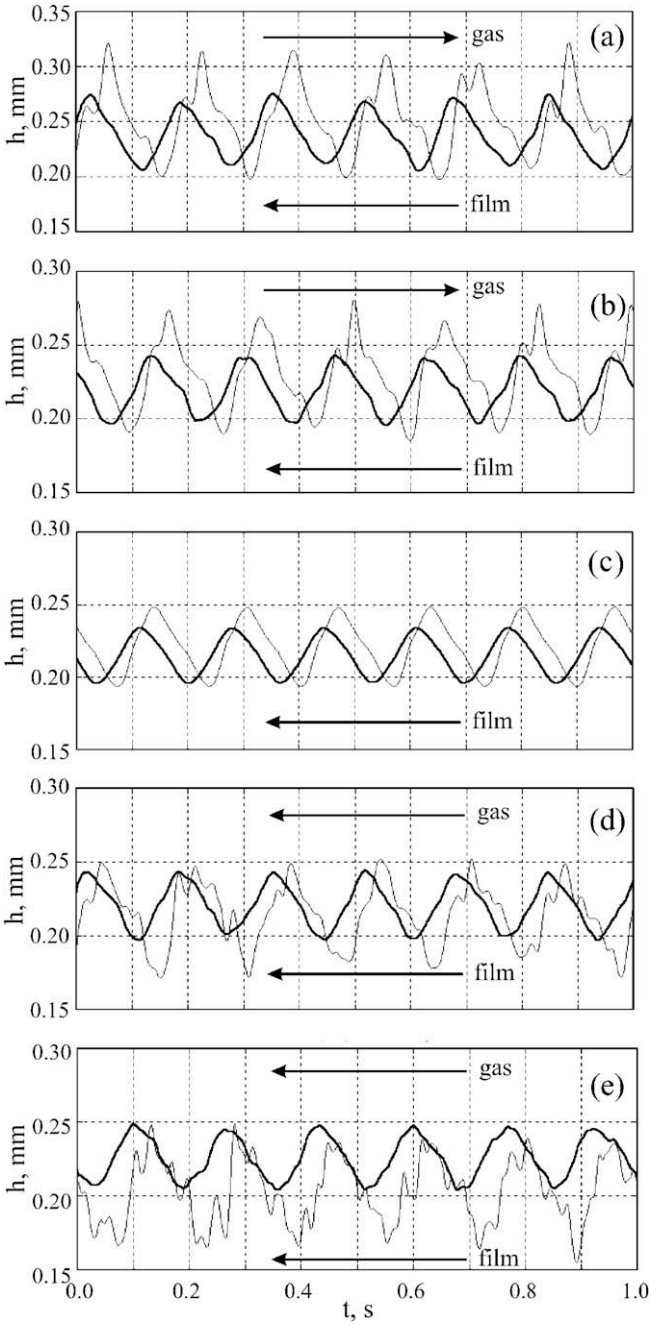

Fig. 3. Wave profiles at different velocities of gas stream. Water, Re = 40. (a and b) Countercurrent flow with gas velocity 7.3 m/s and 5.1 m/s; (c) free falling film; (d and e) cocurrent flow with gas velocity 5.1 m/s and 8.0 m/s. Bold line represents signal of upstream sensor.

2.3. Determination of region appropriate for measurement of linear waves characteristics

Experimental study of linear waves characteristics is complicated by small length of the zone where the measurements are possible: this zone must start downstream the region of film flow stabilization (see Fig. 2) and end in the location where waves become significantly nonlinear. It is worth noting that the concept of stabilization length is rather conditional because this length is usually defined as a distance from the distributor to the location

Table 1
Liquid properties and tested regimes.

Liquid	$\rho \times 10^3$ (kg/ m^3)	$\sigma/\rho \times 10^6$ (m^3/s^2)	$\nu \times 10^6$ (m^2/s)	Re	Gas velocity, V_g (m/s)
Water	1.0	72.0	1.0	24; 40	8.0; 5.1; 0; −5.1; −7.3
Water–glycerin solution # 1 (WGS1)	1.07	65	2.1	24; 40; 70; 105; 124	7.3; 5.1; 0; −5.1; −7.3; 7.3; 5.1; 0; −5.1
Water–glycerin solution # 2 (WGS2)	1.1	61	3.45	10	7.3; 5.1; 0; −5.1; −7.3

where the film average characteristics (e.g., film thickness) deviate from the equilibrium level by a small but finite value. However, it is not generally determined at what magnitude of this deviation there are no significant effects on wave characteristics anymore. Influence of this deviation on dispersion relations is studied in Appendix B on the base of integral approach. Both c and α values appear to decrease with increasing of level of this deviation. Therefore, in our experiments, we made sure that sensors for obtaining dispersion relations belong to the zone of equilibrium flow in the following way: the phase velocity of waves is determined for several frequencies for the base between sensors 1 and 2, 2 and 3, 3 and 4. If the dependencies of the phase velocity on frequency coincide at least for two pairs of neighboring sensors (for example, for pairs 1–2 and 2–3), we assume that the sensors are located in the area of hydrodynamically stabilized film flow. As an example, in Fig. 4 the dependencies of phase velocity upon frequency are shown for three bases at two different liquid flow rates when the first sensor was placed 10 mm downstream the distributor outlet. Fig. 4a presents the dispersion curves for water at Re = 40. It can be seen that the velocities determined for the bases 1–2 and 2–3 match well, so sensors 1, 2, and 3 are in the zone of stabilized flow. As for the pair 3–4, a slightly lower velocity is observed for the frequency range of 28–40 Hz, and this can be explained by the manifestation of nonlinear effects, because exactly in this frequency range the waves with maximal growth exist. The same dependencies for water at Re = 124 are plotted in Fig. 4b. Obviously, there are no grounds to assume that even one pair of sensors is in the zone of stabilized flow. Hence the sensors should be placed at greater distance from the distributor outlet. Depending on the Reynolds number of film flow, the first sensor was placed at the distance 10–45 mm downstream the inlet. The other sensors were placed along vertical line with the step of 15 mm downstream.

Since the growing waves tend to evolve quickly to the nonlinear mode, the special emphasis was put on fulfillment of conditions when the contribution of nonlinear effects is smaller than the measurement error.

The wave was considered as a linear one if its spatial increment and phase velocity were independent of the amplitude for the case of nonzero spatial increment. The measurements were performed at different levels of wave excitation, and during processing the wave was considered as linear, exponentially growing wave in one of the following cases:

(1) For positive spatial increment, the magnitudes of the increment and phase velocity are the same for two adjacent sets of sensor pairs.
(2) For positive spatial increment, the magnitudes of the increment and phase velocity are independent of excited wave amplitude for the pair of sensors, whose data are used for derivation of dispersion dependencies.

The use of described criteria gives us an upper limit for wave excitation level.

The minimal level for the wave excitation must provide a reasonable signal-to-noise ratio and is discussed in the next subsection.

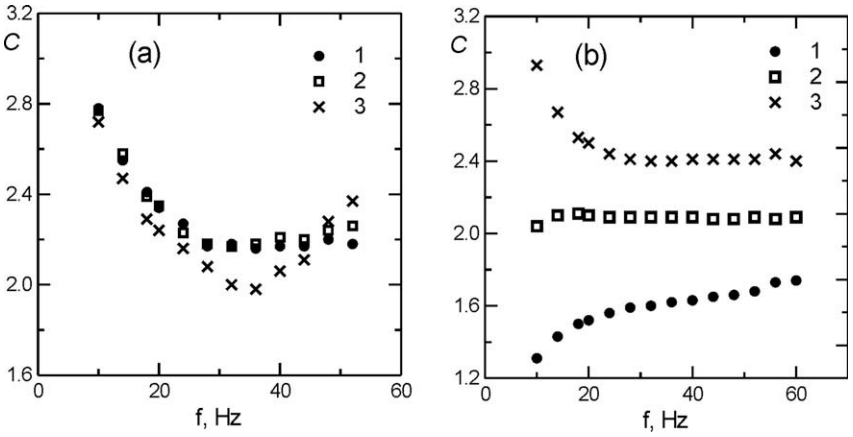

Fig. 4. Dependencies of phase velocity upon frequency of excitation. Water. (a) Re = 40, (b) Re = 124. 1 – 1–2 sensors; 2 – 2–3 sensors; 3 – 3–4 sensors. The first sensor is installed 10 mm downstream the distributor outlet.

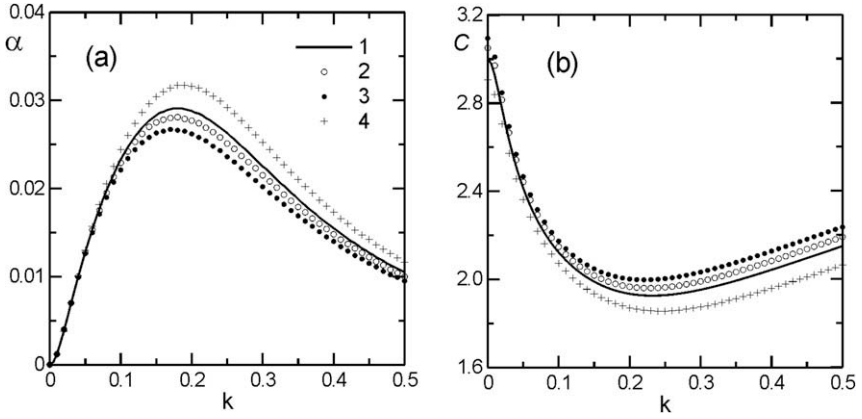

Fig. 5. Influence of channel curvature on dispersion dependencies, WGS1 at Re = 40, (a) increments, (b) phase velocities. 1 – $R = \infty$ (flat plane), 2 – $R = 7.5$ mm (our experiments), 3 – $R = 4$ mm; 4 – $R = -4$ mm (flow on outer side of cylinder).

2.4. Measurements accuracy and additional considerations

For free falling film flow, one of the main sources of noise is the low-frequency vibrations of man-caused origin. Under experimental conditions the vibration-produced noise has rather small amplitude and low frequency. In presence of turbulent air flow the noise spectrum becomes wider. For the maximum air flow rates the noise level can grow by factor of hundred, drastically reducing the signal-to-noise ratio. During data processing, the minimal possible level of excitation was taken that provided at least 30-times overwhelming of first harmonic of signal over the average level of noise spectrum in the adjoining spectral domain. This signal-to-noise ratio ensured the error in measurement of spatial increment smaller than 8%, and the error for phase velocity measurement smaller than 3% (for maximal air velocity for the entire range of excitation frequencies). For the film flow without air blowing, the signal-to-noise ratio was much better, and the maximal errors did not exceed 4% and 2%, respectively.

The finite size of the experimental sensors results in integrating of film thickness for the area, comparable with sensors size. This leads to essential lowering in signal level for high values of wave number and impedes obtaining reliable results for high frequencies of excitation. However, such influence is unessential for the moderate frequencies. For example, the estimated wavelength for dimensionless wave number $k = 0.15$ is equal to 8 mm for film flow of water at Re = 40, so the size of used probe provides enough degree of localization. Here $k = 2\pi \cdot h_0/\lambda$, and λ is the wavelength.

When experimental results obtained for film falling on the inner/outer side of the tube are compared with simulation data, there usually arises the question about the influence of channel curvature radius R on wavy characteristics of film flow. This influence was estimated on the basis of integral approach in cylindrical coordinates. The equation was derived in the same manner as it was done by Alekseenko et al. (1994) for Cartesian coordinates. The estimation have shown that for our experiments the curvature of working channel should lead to some increase in phase velocity and decrease in wave increment. However, for tested flow regimes these changes do not exceed experimental error. The effect of channel curvature radius on spatial increment and wave phase velocity is shown in Fig. 5 for WGS1 at Re = 40.

3. Measurement results and comparison with theory

Figs. 6–9 present measured wave characteristics of film flow in the form of relationships $c(k)$ and $\alpha(k)$. The experimental points are presented only for utmost values of superficial gas velocity V_g: −7.3 and 7.3 (8.0) m/s. The dependencies for intermediate values of V_g (−5.1 and 5.1 m/s) do not provide any additional information and they are always in the position between the cases of no air flow and maximal velocity of gas.

For the Reynolds number higher than 70, the maximal gas velocity for countercurrent flow was −5.1 m/s, since at $V_g = -7.3$ m/s transition to flooding begins. Calculation results based on Orr–Sommerfeld equation are also shown in these figures.

Analysis of experimental dependencies shows that the following regularities may be observed for all tested experimental regimes:

For any gas flow direction, a frequency region exists where the increment is higher than that for free falling film, and the effect of countercurrent gas flow is higher than that of cocurrent gas flow.

Nature of experimental $\alpha(k)$ – dependencies indicates that for countercurrent gas flow the increment growth is accompanied by narrowing instability range of k, at the same time the value of k for waves of maximal growth is rather conservative value. Contrary, for the cocurrent flow, the increment growth is accompanied by an expansion of instability range of k. An increase of the value of k for waves of maximal growth takes place in this case.

The wave phase velocity, especially for maximal growth waves, is very sensitive to the velocity of countercurrent gas flow and decreases rapidly with an increase in the gas velocity. The effect of cocurrent gas flow on wave phase velocity is weak and only a slight growth of phase velocity takes place. In general, the calculated patterns are rather good in description of described above regularities. The theoretical and experimental curves of $\alpha(k)$ are quite close at Re < 70 and for range $k < 0.15$. For this range of Re, the main discrepancy between theory and experiment is observed at high frequencies, where the experimental values for increment are much lower than in theory. The possible reason for this could be the low-frequency fluctuations of the film thickness disregarded in the theory but inevitably present in experiment. Such fluctuations lead to modulation of the excited waves. The estimation performed in Appendix C shows that allowance for fluctuation of film thickness in theory leads to more rapid decrease of the increment with the growth of frequency and makes it possible to explain the divergence between theoretical and experimental dispersion curves at high frequencies.

For Re > 70 the considerable exceeding of the experimental values of increment above the calculations is observed (Fig. 9a and b). The possible explanation is that the Benjamin model is not valid at high Re, because a thick film has more bad correspondence to a rigid unmovable wall.

The observed discrepancy between experimental and theoretical curves for $c(k)$ is almost independent of frequency and has a

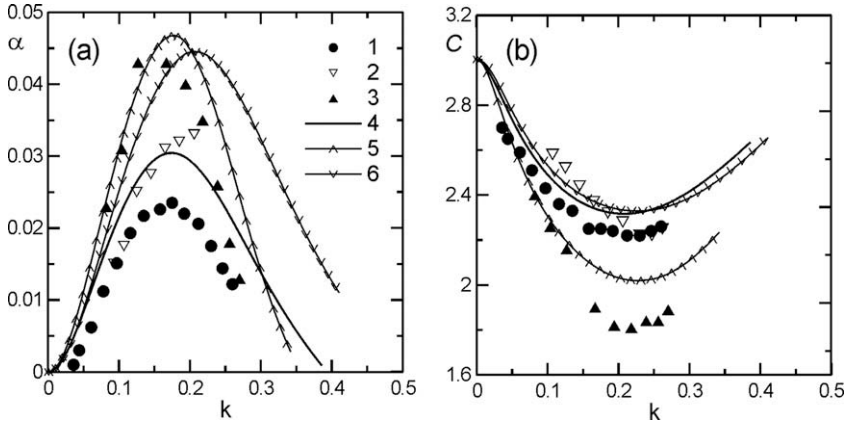

Fig. 6. Dispersion dependencies for WGS2 at Re = 10; (a) increments (b) phase velocities. Experiments: 1 – $V_g = 0$; 2 – $V_g = -7.3$ m/s (countercurrent flow), 3 – $V_g = 7.3$ m/s (cocurrent flow). Calculations: 4 – $V_g = 0$; 5 – $V_g = -7.3$ m/s; 6 – $V_g = 7.3$ m/s.

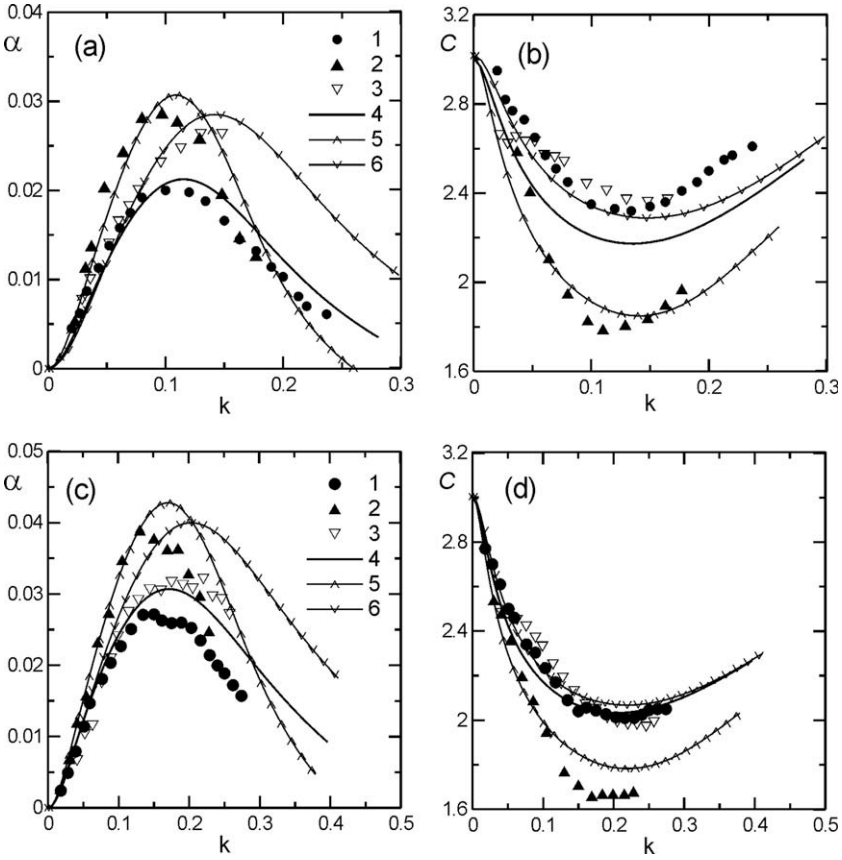

Fig. 7. Dispersion dependencies for Water and WGS1 at Re = 24; (a and b) increments and phase velocities for water. Experiments: 1 – $V_g = 0$; 2 – $V_g = -7.3$ m/s; ▽ – $V_g = 8.0$ m/s. Calculations: 4 – $V_g = 0$; 5 – $V_g = -7.3$ m/s; 6 – $V_g = 8.0$ m/s. (c and d) Increments and phase velocities for WGS1. Experiments: 1 – $V_g = 0$; 2 – $V_g = -7.3$ m/s; 3 – $V_g = 7.3$ m/s. Calculations: 4 – $V_g = 0$; 5 – $V_g = -7.3$ m/s; 6 – $V_g = 7.3$ m/s.

systematic nature. For water tests, experimental points are higher than calculated (see Figs. 7b and 8b) and the opposite is true for WGS (see Figs. 6, 7b and 7–9d). This systematic difference increases with Reynolds number. For water this difference is 5% at Re = 24 and 10% at Re = 40; for WGS 5% at Re = 10 and increases up to 20% at Re = 125.

4. Conclusions

The experimental study of the stability of vertically falling film in the presence of the cocurrent and countercurrent gas flow has been performed for the wide range of film Reynolds number $10 \leqslant \mathrm{Re} \leqslant 125$ and gas velocity $-7.3\ m/s \leqslant V_g \leqslant 8.0\ m/s$. The dispersion relations have been obtained for the developing small amplitude two-dimensional waves. Since the region of linear development of the waves is very short in downstream direction and located close to the inlet region, special attention was given to postulate and fulfill the criteria, which makes it possible to treat the results obtained as related to the characteristics of linear waves in the region of hydrodymamically stabilized film flow.

The independence of phase velocity from the downstream distance was selected as the criterion of matching the measurement area with the region of stabilized film flow, and the independence of the nonzero spatial increment from the amplitude of excited waves was selected as the criterion of wave's linearity.

It is shown experimentally that for any direction of gas flow the wave increment in the vicinity of maximal growth waves is higher than for free falling films. The wave phase velocity, especially for maximal growth waves, is quite sensitive to the velocity of countercurrent gas flow and only slightly increases with the velocity of cocurrent gas flow.

The experimental results were compared with results obtained by direct solution of Orr–Sommerfeld equation based on separate problem formulation for liquid film and gas flow and quasi-laminar model of Benjamin for turbulent gas flow. It is shown that such approach makes it possible to describe adequately the stability of joint flow of liquid film and turbulent gas flow at $\mathrm{Re} \leqslant 70$.

The possible origins of the discrepancy between experiments and modeling have been analyzed including liquid film transversal curvature and presence of uncontrolled low-frequency fluctuations of film surface.

Appendix A. Stability of the film flow on the basis of Orr–Sommerfeld equation

Used quasi-laminar model of a turbulent stream of gas is based on the following assumptions: (1) the film surface is considered as the immobile wavy rigid surface with wave amplitude much less than film thickness; (2) interface disturbances are small for gas flow, and the disturbed gas flow can be described by linearized equations (Benjamin, 1959). The model permits to calculate the disturbances of the shear and normal stresses at the interface due to pulsations of the film thickness. With this approach a small disturbance in the stream function of type $\Psi(x,y,t) = \phi(y)\exp(ik(x-ct) + \beta t)$ for stationary liquid film flow is examined, which results in Orr–Sommerfeld equation for $\phi(y)$ (Demekhin et al. 1989; Aktershev and Alekseenko 1996):

$$\varphi'''' - 2k^2\varphi'' + k^4\varphi = ik\mathrm{Re}\cdot((u_0 - \tilde{c})(\varphi'' - k^2\varphi) - U_0''\cdot\varphi)$$

with boundary conditions

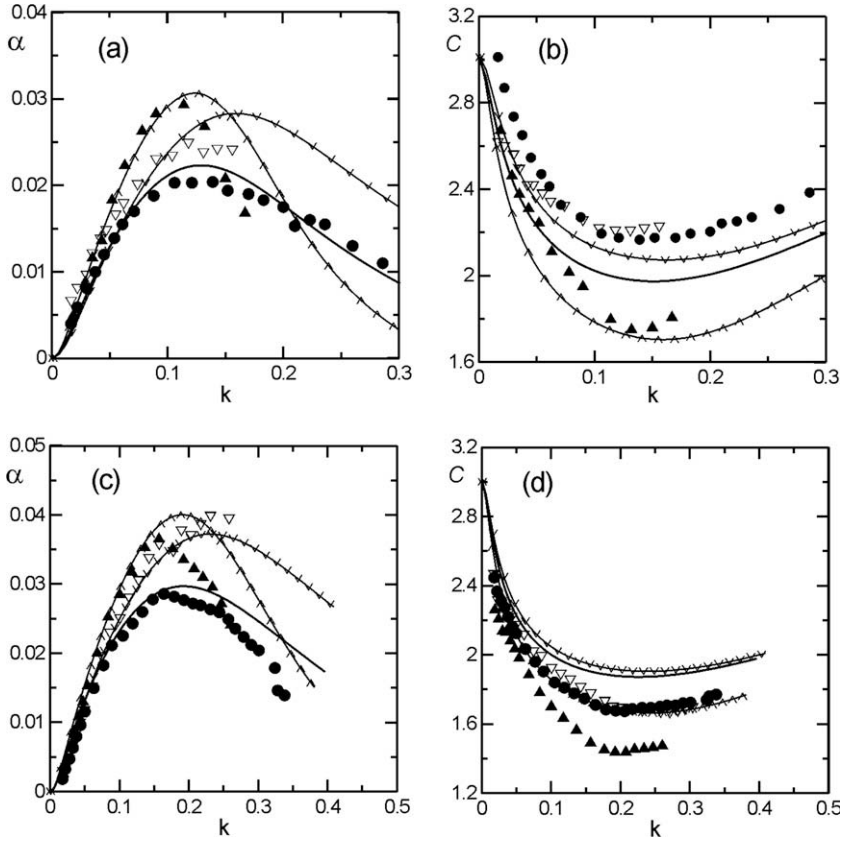

Fig. 8. Dispersion dependencies for Water and WGS1 at Re = 40; for notation see Fig. 7.

$$\text{at } y=0 \text{ (wall)}: \ \varphi(0)=0, \ \ \varphi'(0)=0$$
$$\text{at } y=1 \text{ (interface)}:$$
$$\frac{c^*}{(c^*k^2-(3+kr\bar{T}))}\varphi''(1)+\varphi(1)=0, \ \ ic^*\varphi'''(1)=kc^*(\mathrm{Re}c^*+3ki)\varphi'(1)-kE\varphi.$$

Here $U_0 = 3(y-y^2/2)+ry$ is the undisturbed film velocity, $r = 3\tau_{s0}/\rho g h_0$ is the undisturbed dimensionless shear stress at the interface, $\tilde{c} = c + i\beta/k$ is the complex velocity of wave, $c^* = \tilde{c} - r - 3/2, E = 3\mathrm{We}\cdot k^2 - r(\mathrm{Re}\cdot c^* + k\bar{F}), \bar{T} = T_R - iT_I, \bar{F} = F_R - iF_I$ are the complex amplitudes of shear and normal gas stresses at the interface, $\mathrm{Re}_0 = gh_0^3/3\nu^2, \mathrm{We} = (3\mathrm{Fi})^{1/3}/\mathrm{Re}_0^{5/3}$ is the Weber number, $\mathrm{Fi} = \sigma^3/\rho^3 g\nu^4$ is the film number.

Demekhin (1981) presented the calculated stress disturbances T_R, T_I, F_R, F_I as functions of dimensionless variable $R_g = \sqrt{\tau_{s0}/\rho_g}/k\nu_g$, where ρ_g, ν_g are density and kinematic viscosity of gas, τ_{s0} is undisturbed shear stress at the interface. These functions were used at the solution of the Orr–Sommerfeld equation for a finding c, β. The value τ_{s0} can be determined from the drag coefficient C_g, assuming $\tau_{s0} = C_g\cdot\rho_g U|U|/2$, where $U = V_g - u_{s0}$ is the relative gas velocity. The values of drag coefficient for a smooth film surface measured by Hanratty and Engen (1957) are rather close to the coefficient for a dry wall. Since in the measurement section the amplitude of excited waves is low in comparison with the thickness of laminar sublayer in gas flow (e.g., Hewitt and Hall Taylor 1970), it is reasonable to consider the film as a smooth one and to take the formula for drag coefficient $C_g = 0.08/\mathrm{Re}_g^{0.25}$ (Blauzius law for smooth wall). Here $\mathrm{Re}_g = |U|\cdot D/\nu_g$ is the Reynolds number for gas. Since under current experimental conditions the effect of gas flow on film velocity is low, one can take $u_{s0} = gh_0^2/2\nu$.

A spatial increment of the surface disturbance α was calculated through relation of Gaster (1962): $\alpha = \beta/(c + k\frac{dc}{dk})$.

Appendix B. Dispersion relationships for the bottom part of the region of hydrodynamic stabilization of film flow

After the liquid film leaves the distributor, the profile of flow velocity rearranges from an equilibrium profile in the gap to the equilibrium flow on a vertical wall. Several authors (Stucheli and Ozisik, 1976; Gimbutis, 1988; etc.) solved the problem of flow rearrangement analytically, in approximation of self-similar velocity profile. Certainly, the real velocity profile in the inlet region is different (see, for example, simulation results of Cerro and Whitaker (1971)), however the substantial difference between exact numerical and approximate analytical solutions takes place only in the close vicinity of the distributor. From the methodological point of view we are interested in wave characteristics in the bottom part of flow stabilization zone (where the film thickness is not very different from the equilibrium level), so we will write down the dispersion relationships in the framework of integral approach assuming a parabolic flow profile and using the existing analytical solution. In this case the solution in the inlet region is as follows (Alekseenko et al., 1994):

$$x = \frac{\mathrm{Re}}{15}\left(2\sqrt{3}arctg\frac{2h+1}{\sqrt{3}} - 2\sqrt{3}arctg\frac{2h_i+1}{\sqrt{3}} + \ln\frac{(1-h)^2(1+h_i+h_i^2)}{(1-h_i)^2(1+h+h^2)}\right), \quad (1)$$

where x, h_i and h are, respectively, the distance from the distributor exit, slot thickness and film thickness, which are made dimensionless using Nusselt film thickness.

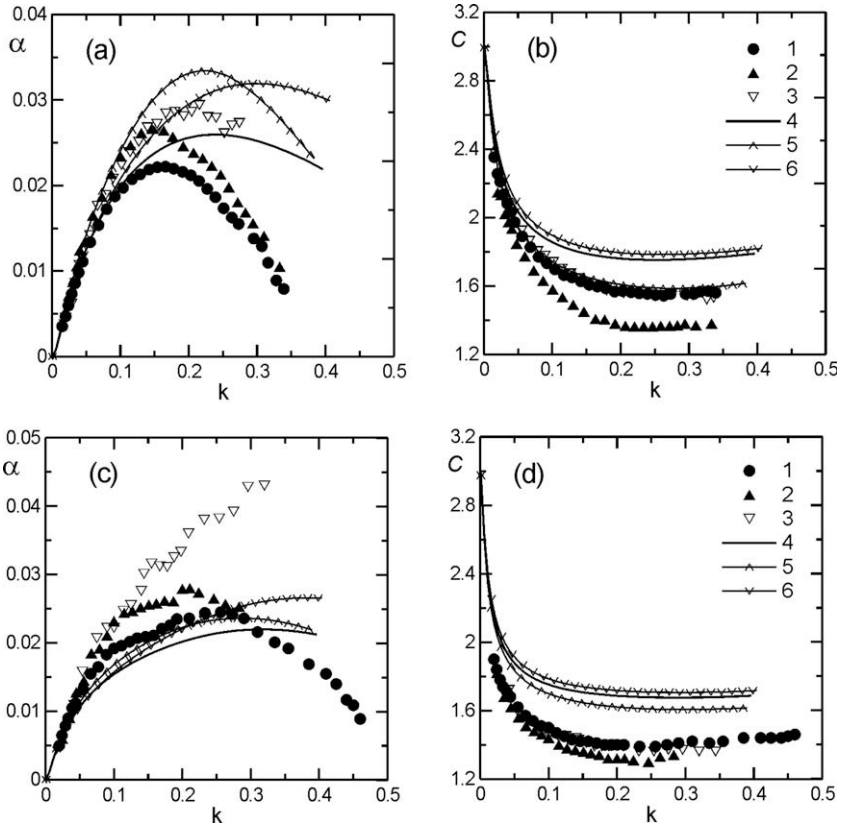

Fig. 9. Dispersion dependencies for WGS1. (a), (b) increments and phase velocities at Re = 70. Experiments: 1 – $V_g = 0$; 2 – $V_g = -7.3$ m/s; 3 – $V_g = 7.3$ m/s. Calculations: 4 – $V_g = 0$; 5 – $V_g = -7.3$ m/s; 6 – $V_g = 7.3$ m/s. (c and d) Increments and phase velocities at Re = 125. Experiments: 1 – $V_g = 0$; 2 – $V_g = -5.1$ m/s; 3 – $V_g = 7.3$ m/s. Calculations: 4 – $V_g = 0$; 5 – $V_g = -5.1$ m/s; 6 – $V_g = 7.3$ m/s.

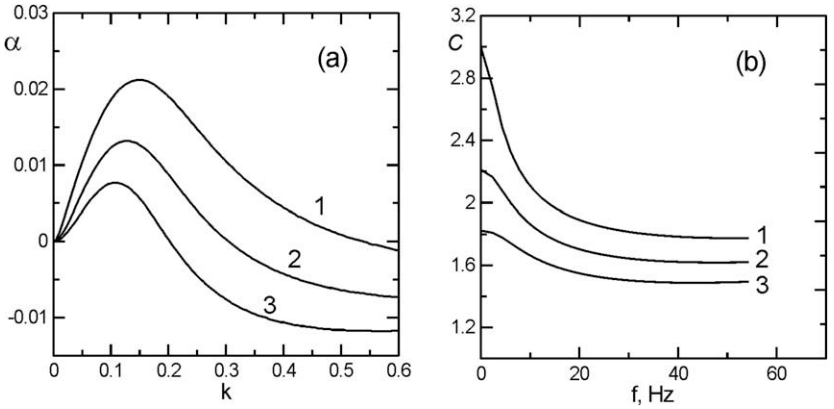

Fig. 10. Influence of inlet region film thickness deviation from the equilibrium level on wave characteristics. (a) Increments for film flow of water at Re = 40; (b) phase velocities for film flow of water at Re = 124. 1 – $\varepsilon = 0$; 2 – $\varepsilon = 0.1$; 3 – $\varepsilon = 0.2$.

Presenting the film thickness in the form $h = 1 + \varepsilon$, where ε is a small deviation of thickness from the Nusselt thickness for stabilized flow, and keeping in Eq. (1) the terms of first order, we obtain:

$$\frac{\partial \varepsilon}{\partial x} = -\frac{7.5}{\mathrm{Re}}\varepsilon. \tag{2}$$

The relation Eq. (2) was used to modify the integral form of momentum and continuity equations, reliable for moderate Re (see, e.g., Alekseenko et al., 1994). The problem of stability of this modified system to small disturbances $H \sim \exp(ikx - ikct + \alpha x)$ may be solved in standard manner to obtain the following system of dispersion relations:

$$\begin{aligned} &4\mathrm{We}(1+\varepsilon)\alpha^3 + \alpha(2.4(1-2\varepsilon) - 2.4(1-\varepsilon)c - 4\mathrm{We}(1+\varepsilon)k^2) \\ &+ \frac{3}{\mathrm{Re}}(1+4\varepsilon)(3(1-4\varepsilon) - c) = 0, \mathrm{We}(1+\varepsilon)\alpha^4 + \alpha^2(1.2(1-2\varepsilon) \\ &- 6\mathrm{We}(1+\varepsilon)k^2) + \alpha\frac{9}{\mathrm{Re}} - k^2(c^2 - 2.4(1-\varepsilon)c + 1.2(1-2\varepsilon)) \\ &+ \mathrm{We}(1+\varepsilon)k^4 = 0. \end{aligned} \tag{3}$$

The results of spatial increment calculation for WGS1 at Re = 40 are plotted in Fig. 10a. It is easy to see that increment decreases with growth of ε, and for the upper limit of experimental frequency range, i.e., for $k = 0.2$–0.4, this decrease is more significant than for small k. Thus, the region of stabilization is equal to a low-frequency filter. For broadband noise generated by turbulent gas flow, this

behavior of dispersion curve in the inlet region results in a serious decrease of signal-to-noise ratio for high frequencies. This puts additional limitations on measurements at high frequencies of excitation.

The results for calculation of phase velocity for water at Re = 124 are presented in Fig. 10b. Although calculations are approximate, and the measurement base in experiment is comparable to the length of stabilization zone, these calculation curves (as well as experimental curves in Fig. 4b) indicate that wave phase velocity increases for all the frequencies with a distance from the distributor. This trait was used as a base for the method of ensuring that sensors are placed in the zone of equilibrium flow.

Appendix C. Effect of fluctuations of average film thickness on characteristics of excited waves

In a real experimental signal, the noise component always exists caused by external sources of vibration and turbulent pulsations of gas flow. Therefore, in real conditions the free film surface is always disturbed, and this definitely changes the wave characteristics of flow.

The effect of such disturbance is demonstrated in Fig. 11. Fig. 11a shows film thickness for a free falling liquid film with high excitation frequency under the influence of 7 Hz external uncontrollable vibration source. The normalized spectrum of this signal is shown in Fig. 11b. It is easy to see in spectral domain, that this low-frequency oscillation creates modulation of high-frequency signal, and, thus, decreases the wave energy at the excitation frequency. Besides, the bold line in Fig. 11a shows the result of low-frequency filtration of a signal, giving the idea on the level of fluctuation causing by this modulation. In this case the amplitude of fluctuation does not exceed 1% of the average film thickness.

A detailed study of the evolution of waves from noise is carried out by Chang et al. (2002). In particular, the authors showed that interaction of developed waves leads to appearance of low-frequency component that modulates waves of fundamental frequency. To avoid misunderstanding, it should be noted that in present paper the modulation from low-frequency external vibrations is considered.

Fig. 11c and d shows the signal, its spectrum and results of low-frequency filtration for wave excited on film blown by cocurrent gas flow. With gas flow the fluctuation of film thickness appears to have a wide spectrum and become more intensive. Since fluctuations are actually irregular waves developing on the film surface, their level depends on experimental conditions. The processing of experimental data demonstrates that the relative level of fluctuations δ in the measurement zone decreases with a growth of Re and increases with a growth of gas velocity. For example, for a free film flow the amplitude of fluctuations was less than 0.5–2.0% of the average film thickness, but at the gas velocity of 5.1 m/s it increases up to 4–7%, and at maximal velocity in some cases it was as high as 10–12 %. The accurate account of the impact of film thickness fluctuation on characteristics of excited waves is an extremely complex problem. However the estimation can be made for a quasi stationary approximation, assuming that all fluctuations are low-frequency, but the current values of phase velocity and increment of excited waves are the same as for a smooth film with thickness $h = h_0(1 + \delta)$, where h_0 is the average value of film thickness, and $\delta(t)$ is its current fluctuation. Let the signal on the top sensor is $A_1 = \exp(-i2\pi ft)$, then on the downstream sensor the signal takes the form: $A_2 = \exp(-i2\pi ft + ikL + \alpha L)$.

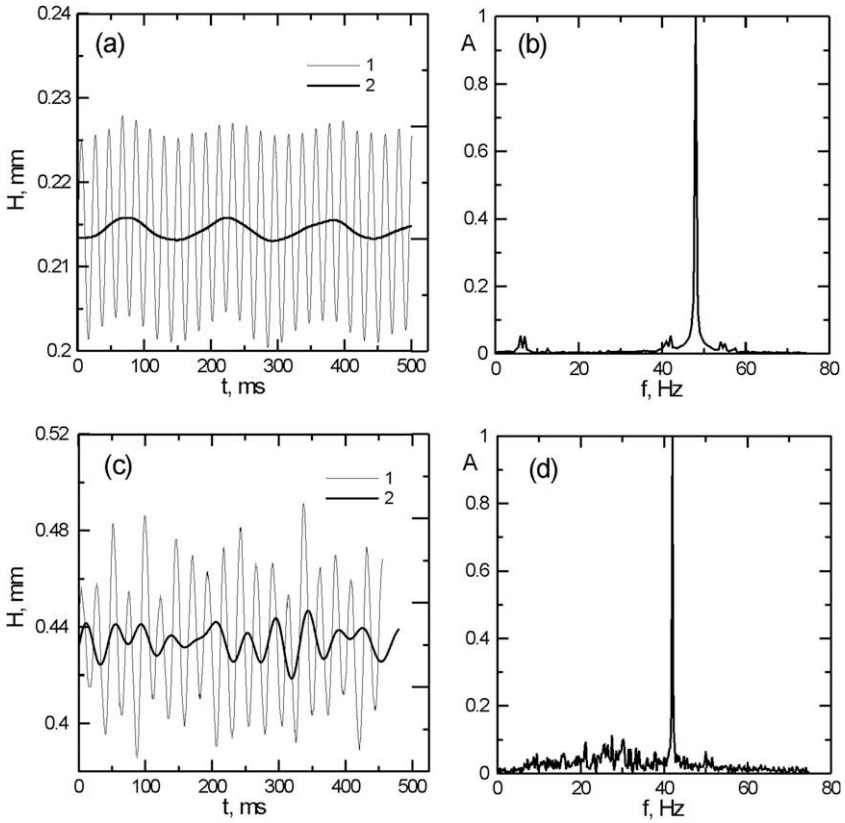

Fig. 11. Excited waves (1), low-frequency fluctuations of film thickness (2) and normalized spectra of signals for gravitational film flow of water at Re = 40 with presence of external low-frequency source of vibration (a and b) and for cocurrent film flow of WGS1 at Re = 70 and V_g = 7.3 m/s (c and d).

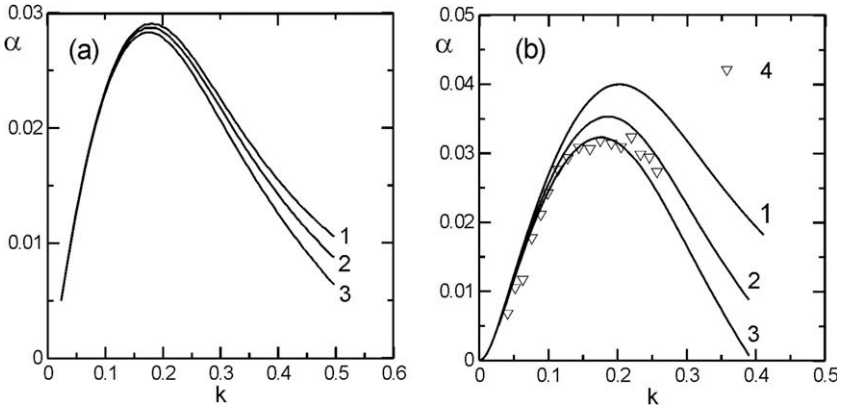

Fig. 12. Effect of fluctuation of film thickness on increment. (a) For free falling film of WGS1 at Re = 40. 1 – $\delta = 0$; 2 – $\delta = 2\%$; 3 – $\delta = 3\%$. The relative level of fluctuation in experiment does not exceed 2%. (b) For film flow of WGS1 at Re = 24 and cocurrent gas flow with velocity of 7.3 m/s. 1 – $\delta = 0$; 2 – $\delta = 7\%$; 3 – $\delta = 9\%$; 4 – experiment ($\delta \sim 7$–9%).

Here $k = k(h)$ is the wave number; $\alpha = \alpha(h)$ is the spatial increment.

Obviously, the signal from the downstream sensor has the amplitude and phase modulation. Setting up the modulation amplitude, we can calculate directly the signal on the downstream sensor. After its processing in the same manner as for the experimental signal, we can see how the fluctuations affect the wave characteristics. For free film flow and moderate Re, this estimation can be done easily from the dispersion relationships obtained on the basis of integral equations. The result of this calculation at several fluctuation levels is shown in Fig. 12a. It can be concluded that existence of fluctuations decreases the increment, and this effect is more pronounced at shorter wavelengths. For a joint film-gas flow, similar qualitative estimation requires unjustifiably huge volume of computations, but in the framework of integral approach with some simplifying assumptions, it can be shown that for the tested regimes the main effect is due to phase modulation of the signal (because for the studied frequency range $|\partial k/\partial h| \gg |\partial\alpha/\partial h|$). Therefore, in our calculations we can use only the relationship for $k(h)$ and take a constant increment $\alpha(h_0)$. Taking into account that for a cocurrent flow the phase velocity of waves is rather close to wave velocity on a free falling film, we can use the same relationship for $k(h)$ as for a free falling film and use $\alpha(h_0)$ obtained as described in Appendix A. The result of this calculation with the experimentally determined level of fluctuation is shown in Fig. 12b. It can be seen that a strong decline in increment at high frequencies may be explained by a high level of fluctuations.

References

Aktershev, S.P., Alekseenko, S.V., 1996. Interfacial instabilities in an annular two-phase flow. Russ. J. Eng. Thermophys. 6 (4), 307–320.

Alekseenko, S.V., Nakoryakov, V.E., Pokusaev, B.G., 1994. Wave Flow of Liquid Films. Begell House, New York.

Alekseenko, S.V., Nakoryakov, V.E., 1995. Instability of a liquid film moving under the effect of gravity and gas flow. Int. J. Heat Mass Transfer 38, 2127–2134.

Asali, J.C., Hanratty, T.J., 1993. Ripples generated on a liquid film at high gas velocities. Int. J. Multiphase Flow 19, 229–243.

Benjamin, T.B., 1957. Wave formation in laminar flow down an inclined plane. J. Fluid Mech. 2, 554–574.

Benjamin, T.B., 1959. Shearing flow over a wavy boundary. J. Fluid Mech. 6 (2), 161–205.

Cerro, R., Whitaker, S., 1971. Stability of falling liquid film. Chem. Eng. Sci. 26 (5), 742–745.

Chan Van Chan, Shkadov, V.Ya., 1979. Instability of the layer of viscous liquid under the action of the boundary flow of the gas. Izv. AN SSSR, Mekh. zhidkosti i gaza. 2, 28–36.

Chang, H.C., Demekhin, E.A., 2002. Complex wave dynamics of thin films. Elsevier.

Chang, H.-C., Demekhin, E.A., Saprikin, S.S., 2002. Noise-driven wave transitions on vertically falling film. J. Fluid Mech. 462, 255–283.

Cheng, M., Chang, H.-C., 1995. Competition between subharmonic and sideband secondary instabilities on a falling film. Phys. Fluids 7 (1), 34–54.

Chu, K.J., Dukler, A.E., 1974. Statistical characteristics of thin wavy films. AIChE J. 20 (4), 695–706.

Cohen, L.S., Hanratty, T.J., 1968. Effect of waves at a gas–liquid interface on a turbulent air flow. J. Fluid Mech. 31, 467–479.

Craik, A.D.D., 1966. Wind-generated waves in liquid films. J. Fluid Mech. 26, 369–392.

Demekhin, E.A., 1981. Nonlinear waves in fluid film, carried along by the turbulent gas flow. Izv. AN SSSR, Mekh. zhidkosti i gaza. 2, 37–42 (in Russian).

Demekhin, E.A., Tokarev, G.Yu., Shkadov, V.Ya., 1989. Instability and non-linear waves between vertical liquid film and countercurrent turbulent gas flow. Teor. Osn. Khimich. Tehnolog. 23 (1), 64–70 (in Russian).

Gaster, M., 1962. A note on the relation between temporarily increasing and spatially increasing disturbances in hydrodynamic stability. J. Fluid Mech. 14, 222–224.

Gimbutis, G., 1988. Heat Transfer in Gravitational Flow of Liquid Film (in Russian) Vilnyus, Mokslas.

Guguchkin, V.V., Demekhin, E.A., Kalugin, G.N., Markovich, E.E., Pikin, V.G., 1975. Wave flow of co-current gas–liquid film. Izv. AN SSSR, Mekh. zhidkosti i gaza. 4, 174–177 (in Russian).

Guguchkin, V.V., Demekhin, E.A., Kalugin, G.N., Markovich, E.E., Pikin, V.G., 1979. On the linear and nonlinear stability of combined plane-parallel flow of liquid film and gas. Izv. AN SSSR, Mekh. zhidkosti i gaza. 1, 36–42 (in Russian).

Hanratty, T.J., Engen, J.M., 1957. Interaction between a turbulent air stream and moving water surface. AIChE J. 3, 299–304.

Hanratty, T.J., 1983. Interfacial instabilities caused by air flow. In: Meyer, R.E. (Ed.), Waves on Fluid Interfaces. Academic Press, New York.

Hewitt, G.F., Hall Taylor, N.S., 1970. Annular Two-Phase Flow. Pergamon Press, Oxford.

Inada, F., Drew, D.A., Lahey Jr., R.T., 2004. An analytical study on interfacial wave structure between the liquid film and gas core in a vertical tube. Int. J. Multiphase Flow 30, 827–851.

Jurman, L.A., McCready, M.J., 1989. Study of waves on thin liquid films sheared by turbulent gas flows. Phys. Fluids A 1 (3), 522–536.

Kapitza, P.L., 1948. Wave flow of thin layers of viscous fluid. Zhurn. Eksper. Teor. Fiz. 18 (1), 3–28 (in Russian).

Kuru, W.C., Sangalli, M., Uphold, D.D., McCready, M.J., 1995. Linear stability of stratified channel flow. Int. J. Multiphase Flow 21, 733–753.

Krantz, W.B., Goren, S.L., 1971. Stability of thin liquid films flowing down a plane. Ind. Eng. Chem. Fundam. 10 (1), 91–101.

Lilleleht, L.U., Hanratty, T.J., 1961. Measurement of interfacial structure for co-current air–water flow. J. Fluid Mech. 11, 65–81.

Liu, J., Paul, J.D., Gollub, J.P., 1993. Measurement of the primary instabilities of film flow. J. Fluid Mech. 250, 69–101.

Liu, J., Schneider, J.B., Gollub, J.P., 1995. Three-dimensional instabilities of film flow. Phys. Fluids 7 (1), 55–67.

Miesen, R., Boersma, B.J., 1995. Hydrodynamic stability of the sheared liquid film. J. Fluid Mech. 301, 175–202.

Miles, J.W., 1959. On the generation of surface wave by shear flow. J. Fluid Mech. 6 (4), 568–598.

Pierson, F.W., Whitaker, S., 1977. Some theoretical and experimental observations of the wave structure of falling liquid films. Ind. Eng. Chem. Fundam. 16 (4), 401–408.

Rossum, J.J., 1959. Experimental investigation of horizontal liquid film thickness. Chem. Eng. Sci. 11, 35–52.

Semenov, P.A., 1944. Flow of liquid in thin layers. Zhurn. Tech. Fiz XIV 7–8, 427–437 (in Russian).

Smith, T.N., Tait, R.W.F., 1966. Interfacial shear stress and momentum transfer in horizontal gas–liquid flow. Chem. Eng. Sci. 21, 63–73.
Stainthorp, F.P., Batt, R.S.W., 1967. The effect of co-current and counter-current air flow on the wave properties of falling liquid films. Trans. Inst. Chem. Eng. 45, 372–382.
Stucheli, A., Ozisik, M.N., 1976. Hydrodynamic entrance lengths of laminar falling films. Chem. Eng. Sci. 31 (5), 369–372.
Tsai, Y.S., Grass, A.J., Simons, R.R., 2005. On the spatial linear growth of gravity-capillary water waves sheared by a laminar air flow. Phys. Fluids 17, 095101.
van Gastel, K., Janssen, P.A.E.M., Komen, G.J., 1985. On phase velocity and growth rate of wind-induced gravity-capillary waves. J. Fluid Mech. 161, 199–216.
Vlachogiannis, M., Bontozoglou, V., 2001. Observation of solitary wave dynamics of film flows. J. Fluid Mech. 435, 191–215.